

Hybrid Schwarz preconditioners for linear systems arising from hp -discontinuous Galerkin method*

Vít Dolejší[†]

Tomáš Hammerbauer*

February 11, 2025

Abstract

We deal with the numerical solution of elliptic problems by the hp -discontinuous Galerkin method. We develop a two-level hybrid Schwarz preconditioner for the arising linear algebraic systems. The preconditioner is additive with respect to the local components and multiplicative with respect to the mesh levels. We derive the hp spectral bound of the preconditioned operator in the form $O((H/h)(p^2/q))$, where H and h are the element sizes of the coarse and fine meshes, respectively, and p and q are the polynomial approximation degrees on the fine and coarse meshes. Further, we present a numerical study showing that the hybrid Schwarz preconditioner dominates the additive one from the point of view of the speed of convergence and also computational costs. Finally, the combination with a hp -mesh adaptation for the solution of nonlinear problem demonstrates the potential of this approach.

Keywords: discontinuous Galerkin, two-level hybrid Schwarz preconditioner, hp -adaptation

MSCcodes: 65N55, 65N30, 65N50

1 Introduction

The discontinuous Galerkin (DG) method [13, 17] exhibits a powerful technique for the numerical solution of partial differential equations. In particular, the piecewise polynomial discontinuous approximation is well suited for hp -mesh adaptation which exhibits an excellent strategy for problems with local singularities, material interfaces, and it gives, under some assumption, an exponential rate of convergence. On the other hand, the DG discretization leads to larger (but sparser) algebraic systems in comparison to conforming finite element methods.

Therefore, a development of efficient iterative solvers is demanding. Among many techniques, a prominent role is played by the *domain decomposition* (DD) methods [35, 14, 38, 23] which can use the power of multiprocessor computers. The main idea is to divide the global problem into several subproblems (based on the decomposition of the computational domain) and solve them independently. The transfer of information among the subproblems can be accelerated by considering a global (coarse) problem. More frequent approach is the use of the DD techniques as preconditioners for Krylov space iterative methods, such as the conjugate gradient method.

The domain decomposition techniques for discontinuous Galerkin approximations were considered in many works, let us mention [21, 4, 3, 8, 34, 27], further paper [5] related to super-penalty DG technique, works [24, 25, 10] dealing with hybridizable DG methods, and papers [12, 30, 39, 19] related to balancing domain decomposition by constraints (BDDC) variants of domain decomposition. In particular, we mention papers [6, 7] analyzing the two-level non-overlapping additive and multiplicative Schwarz preconditioners. See also [20, 31] containing an alternative approach when the coarse mesh is created by several subdomains treated in parallel.

*Submitted to the editors DATE.

[†]Charles University, Faculty of Mathematics and Physics, Prague, Czech Republic (vit.dolejsi@matfyz.cuni.cz, hammerbt@karlin.mff.cuni.cz).

In contrary to conforming finite element methods (FEM), the advantage of non-overlapping discontinuous Galerkin domain decomposition approach is that each degree of freedom belongs to only one subdomain, any specific operator at subdomain interfaces need not to be constructed and the coarse operator is defined using the same variational formulation as the original problem.

In this paper, we introduce the *two-level non-overlapping hybrid Schwarz* technique proposed in [32] for FEM, when the preconditioner operator is additive with respect to the local components and multiplicative with respect to the mesh levels. The hybrid Schwarz technique was used in various applications, for example [9, 36, 28].

We present the discretization of a linear elliptic problem using the symmetric interior penalty Galerkin (SIPG) method. Assuming a suitable indexing of mesh elements, the one-level additive Schwarz method is equivalent to the block Jacobi iterative method. Then we introduce the two-level additive and hybrid Schwarz methods, and adapting the techniques from [7], we derive the *hp* spectral bound of the two-level non-overlapping hybrid Schwarz preconditioner which is the first novelty of this paper.

Moreover, we present a detailed numerical study of the convergence of the conjugate gradient (CG) method with the two-level additive and hybrid Schwarz preconditioners. The aim is to achieve the *weak scalability* of the solver, namely the number of iterations of the algebraic solver does not increase when the size of sub-problems is kept fixed. Additionally, we compare both preconditioners from the point of view of the number of floating point operations and number of communications among the computer cores.

Finally, the potential of both techniques is demonstrated by numerical solution of a nonlinear elliptic equation in combination with a mesh adaptation. In particular, the arising nonlinear algebraic system is solved by the Newton method and at each Newton step, the corresponding linear system is solved by CG with the presented preconditioners. The mesh adaptation is carried out by the *anisotropic hp-mesh adaptation* technique from [18], which serves as a test of the robustness of the hybrid and additive preconditioners with respect to *hp*-adaptation and the anisotropy of the mesh elements.

The rest of the paper is the following. In Section 2, we introduce the SIPG discretization of the model problem. In Section 3, we introduce the two-level hybrid Schwarz preconditioner and in Section 4 we derive the corresponding spectral bound. The numerical study demonstrating the performance of the additive and hybrid preconditioners is given in Section 5. Several concluding remarks are given in Section 6.

2 Problem definition

In the following, we use the standard notation for the Lebesgue space $L^2(\Omega)$, the Sobolev space $H^k(\Omega) = W^{k,2}(\Omega)$, and $P^p(M)$ is the space of polynomials of degree at most p on $M \subset \mathbb{R}^d$. Moreover, we use the notation

$$(u, v)_M = \int_M u v \, dx \quad \text{for } M \subset \mathbb{R}^s, \, s = 1, \dots, d. \quad (1)$$

Let $\Omega \in \mathbb{R}^d$, $d = 2, 3$ be a bounded polygonal domain with Lipschitz boundary $\Gamma := \partial\Omega$. Let $f \in L^2(\Omega)$ be a source term and $\mathbf{K} \in \mathbb{R}^{d \times d}$ be a symmetric positive-definite diffusion tensor such that

$$\xi \cdot \mathbf{K} \xi \geq k_0 |\xi|^2 \quad \text{and} \quad |\mathbf{K} \xi| \leq k_1 |\xi| \quad \forall \xi \in \mathbb{R}^d \quad (2)$$

for real values $0 < k_0 \leq k_1$.

We consider the linear model problem with the Dirichlet boundary condition

$$-\nabla \cdot (\mathbf{K} \nabla u) = f \quad \text{in } \Omega, \quad (3a)$$

$$u = u_D \quad \text{on } \Gamma, \quad (3b)$$

where $u : \Omega \rightarrow \mathbb{R}$ is an unknown scalar function defined on Ω , and $u_D \in L^2(\Gamma_D)$. Obviously, problem (3) possesses a unique weak solution.

2.1 DG discretization

Let \mathcal{T}_h be a partition of $\bar{\Omega}$ consisting of a finite number of d -dimensional simplices K with mutually disjoint interiors. The symbol ∂K denotes a boundary of $K \in \mathcal{T}_h$, and $h_K = \text{diam}(K)$ is its diameter. The approximate solution of (3) is sought in the finite dimensional space

$$S_h = \{v \in L^2(\Omega); v|_K \in P^{p_K}(K) \forall K \in \mathcal{T}_h\}, \quad (4)$$

where p_K is local polynomial degree assigned to each $K \in \mathcal{T}_h$. We assume that the ratio of polynomial degrees p_K and $p_{K'}$ of any pair of elements K and K' that share a face (edge for $d = 2$) is bounded.

By Γ_h we denote the union of all faces γ contained in \mathcal{T}_h . Moreover, Γ_h^I and Γ_h^B denotes the union of interior and boundary faces of Γ_h , respectively. For each $\gamma \in \Gamma_h$, we consider a unit normal vector \mathbf{n}_γ , its orientation can be chosen arbitrarily for the interior faces. Symbols $[[v]]_\gamma$ and $\langle v \rangle_\gamma$ denote the jump of v multiplied by \mathbf{n}_γ and the mean value of $v \in S_h$ on $\gamma \in \Gamma_h^I$, respectively. For $\gamma \in \Gamma_h^B$, we put $[[v]]_\gamma = v\mathbf{n}_\gamma$ and $\langle v \rangle_\gamma = v$. If there is no risk of misunderstanding we drop the subscripts γ .

Let $\gamma \in \Gamma_h^I$ and $\gamma \subset \partial K \cap \partial K'$, $K \neq K'$, we set

$$h_\gamma = \max(h_K, h_{K'}), \quad p_\gamma = \max(p_K, p_{K'}). \quad (5)$$

For $\gamma \subset \partial K \cap \Gamma_h^B$, we set $h_\gamma = h_K$ and $p_\gamma = p_K$.

Using (1), we define the forms for $u, v \in S_h$, (cf. [17, Section 4.6] or [11])

$$\begin{aligned} \mathcal{A}_h(u, v) &:= \sum_{K \in \mathcal{T}_h} (\mathbf{K} \nabla u, \nabla v)_K - \sum_{\gamma \in \Gamma_h} \left((\langle \mathbf{K} \nabla u \rangle - \sigma [[u]], [[v]])_\gamma + (\langle \mathbf{K} \nabla v \rangle, [[u]])_\gamma \right), \\ g_h(v) &:= (f, v)_\Omega - \sum_{\gamma \in \Gamma_h^B} \left((\langle \mathbf{K} \nabla v, u_D \mathbf{n}_\gamma \rangle - (\sigma u_D, v)_\gamma) \right), \end{aligned} \quad (6)$$

where the penalty parameter σ is chosen by $\sigma|_\gamma = C_W k_0 p_\gamma^2 / h_\gamma$, $\gamma \in \Gamma_h$, with a constant $C_W > 0$, see [17, Chapter 2]. Then the discrete problem reads.

Definition 2.1. *We say that $u_h \in S_h$ is the approximate solution of (3) by symmetric interior penalty Galerkin (SIPG) method if*

$$\mathcal{A}_h(u_h, v_h) = g_h(v_h) \quad \forall v_h \in S_h. \quad (7)$$

3 Domain decomposition method

We follow the approach from [6, 7], where more details can be found. We consider a non-overlapping domain decomposition of Ω as a set of open sub-domains Ω_i , $i = 1, \dots, N$ such that $\Omega_i \cap \Omega_j = \emptyset$ and $\bar{\Omega} = \cup_{i=1, \dots, N} \bar{\Omega}_i$. The sub-domains Ω_i are constructed as a union of some elements $K \in \mathcal{T}_h$, the corresponding meshes are denoted as $\mathcal{T}_{h,i}$, $i = 1, \dots, N$. We consider the finite dimensional spaces

$$S_{h,i} = \{v \in L^2(\Omega_i); v|_K \in P^{p_K}(K) \forall K \in \mathcal{T}_{h,i}\}, \quad i = 1, \dots, N. \quad (8)$$

Besides the mesh \mathcal{T}_h , we consider a coarser mesh $\mathcal{T}_H = \{\mathcal{K}\}$ which typically consists of polygonal/polyhedral elements \mathcal{K} defined as a union of some $K \in \Omega_i$, $i = 1, \dots, N$. We assume that any $\mathcal{K} \in \mathcal{T}_H$ belongs to only one subdomain Ω_i including the case $\mathcal{K} = \bar{\Omega}_i$ for some $i = 1, \dots, N$. Let $q_{\mathcal{K}} = \min_{K \subset \mathcal{K}} p_K$, $\mathcal{K} \in \mathcal{T}_H$, we define the coarse finite element space (cf. (4))

$$S_{h,0} := \{v \in L^2(\Omega); v|_{\mathcal{K}} \in P^{q_{\mathcal{K}}}(\mathcal{K}) \forall \mathcal{K} \in \mathcal{T}_H\}, \quad (9)$$

and set $H := \max_{\mathcal{K} \in \mathcal{T}_H} H_{\mathcal{K}}$ with $H_{\mathcal{K}} = \text{diam}(\mathcal{K})$, $\mathcal{K} \in \mathcal{T}_H$.

3.1 Local problems

We introduce the restriction operators $R_i : S_h \rightarrow S_{h,i}$, $i = 1, \dots, N$ as $R_i v_h = v_h|_{\Omega_i}$, $i = 1, \dots, N$, $v_h \in S_h$. The corresponding prolongation operators $R_i^\top : S_{h,i} \rightarrow S_h$ are given by $R_i^\top v_h = v_h$ on Ω_i and $R_i^\top v_h = 0$ on $\Omega \setminus \Omega_i$ for $v_h \in S_{h,i}$, $i = 1, \dots, N$. Moreover, since $S_{h,0} \subset S_h$, we define the prolongation operator $R_0^\top : S_{h,0} \rightarrow S_h$ as a standard injection from $S_{h,0}$ to S_h . The restriction operator $R_0 : S_h \rightarrow S_{h,0}$ is given as the dual operator to R_0^\top with respect to the $L^2(\Omega)$ duality.

Furthermore, using (6), we define the *local forms* $\mathcal{A}_{h,i} : S_{h,i} \times S_{h,i} \rightarrow \mathbb{R}$ by

$$\mathcal{A}_{h,i}(u_i, v_i) := \mathcal{A}_h(R_i^\top u_i, R_i^\top v_i), \quad u_i, v_i \in S_{h,i}, \quad i = 0, \dots, N, \quad (10)$$

and the *local projections* $\tilde{P}_i : S_h \rightarrow S_{h,i}$ and $P_i : S_h \rightarrow S_h$ by

$$\mathcal{A}_{h,i}(\tilde{P}_i u, v_i) = \mathcal{A}_h(u, R_i^\top v_i) \quad \forall v_i \in S_{h,i} \quad \text{and} \quad P_i := R_i^\top \tilde{P}_i, \quad i = 0, \dots, N, \quad (11)$$

respectively. Finally, the *two-level additive Schwarz preconditioned operator* reads

$$P_{\text{add},2} := \sum_{i=0}^N P_i. \quad (12)$$

3.2 Algebraic representation

Let $\mathcal{B}_h := \{\varphi_k\}_{k=1}^n$ be a basis of S_h ($n = \dim S_h$), the support of each basis function $\varphi \in \mathcal{B}_h$ is just a one $K \in \mathcal{T}_h$. We assume that the basis functions are numbered such that first we number test functions with support in Ω_1 , then functions with support in Ω_2 , etc.

Then problem (7) is equivalent to linear algebraic system

$$\mathbf{A}\mathbf{u} = \mathbf{g}, \quad (13)$$

where \mathbf{A} , \mathbf{u} , and \mathbf{g} are algebraic representation of \mathcal{A}_h , u_h , and g_h , respectively, with respect to basis \mathcal{B}_h . Similarly, let \mathbf{R}_i and \mathbf{R}_i^\top denote the algebraic representations of the operators R_i and R_i^\top (cf. (3.1)) with respect to \mathcal{B}_h , respectively for $i = 0, \dots, N$. Particularly, the matrices \mathbf{R}_i^\top for $i = 1, \dots, N$ are just extensions of unit matrices of the corresponding sizes by zero blocks and \mathbf{R}_0^\top is given by an evaluation of the basis functions of S_H by basis functions of \mathcal{B}_h , we refer, e.g. [3] for details. Obviously, \mathbf{R}_i are transposed matrices of \mathbf{R}_i^\top for $i = 0, \dots, N$.

Moreover, the algebraic representation of the local bilinear forms $\mathcal{A}_{h,i}$, the operators \tilde{P}_i , P_i from (10)–(11) reads (cf. [21, 6, 7, 20])

$$\mathbf{A}_i = \mathbf{R}_i \mathbf{A} \mathbf{R}_i^\top, \quad \tilde{\mathbf{P}}_i = \mathbf{A}_i^{-1} \mathbf{R}_i \mathbf{A}, \quad \mathbf{P}_i = \mathbf{R}_i^\top \mathbf{A}_i^{-1} \mathbf{R}_i \mathbf{A}, \quad i = 0, \dots, N, \quad (14)$$

and the representation of the additive Schwarz operator $P_{\text{add},2}$ from (12) is

$$\mathbf{P}_{\text{add},2} = \sum_{i=0}^N \mathbf{P}_i = \sum_{i=0}^N \mathbf{R}_i^\top \mathbf{A}_i^{-1} \mathbf{R}_i \mathbf{A} =: \mathbf{N}_{\text{add},2}^{-1} \mathbf{A}, \quad (15)$$

The matrix $\mathbf{N}_{\text{add},2}^{-1}$ is the two-level additive Schwarz preconditioner. Furthermore, we denote the one-level additive Schwarz preconditioner by

$$\mathbf{N}_{\text{add},1}^{-1} := \sum_{i=1}^N \mathbf{R}_i^\top \mathbf{A}_i^{-1} \mathbf{R}_i = \text{diag}(\mathbf{A}_1^{-1}, \dots, \mathbf{A}_N^{-1}). \quad (16)$$

The above matrix-block equality is valid due to the used numbering of basis functions. Finally, we note that \mathbf{P}_i are projections, since, in virtue of (14), we have

$$\mathbf{P}_i^2 = \mathbf{R}_i^\top \mathbf{A}_i^{-1} \mathbf{R}_i \mathbf{A} \mathbf{R}_i^\top \mathbf{A}_i^{-1} \mathbf{R}_i \mathbf{A} = \mathbf{R}_i^\top \mathbf{A}_i^{-1} \mathbf{A}_i \mathbf{A}_i^{-1} \mathbf{R}_i \mathbf{A} = \mathbf{P}_i, \quad i = 0, \dots, N \quad (17)$$

provided that the performance of local solvers \mathbf{A}_i^{-1} is carried out exactly.

3.3 Iterative methods

To have better view in the performance of preconditioner, we consider the (one and two levels) iterative additive Schwarz schemes solving (13). The matrix \mathbf{A} has blocks $\mathbf{A} = \{\mathbf{A}_{ij}\}_{i,j=1}^N$ such that each block \mathbf{A}_{ij} contains entries corresponding to $\mathcal{A}_h(\varphi_k, \varphi_l)$, $k, l = 1, \dots, n$ satisfying $\text{supp}(\varphi_k) \subset \bar{\Omega}_j$ and $\text{supp}(\varphi_l) \subset \bar{\Omega}_i$. Obviously, if $i \neq j$ and Ω_i and Ω_j have no common edge ($d = 2$) or face ($d = 3$) then $\mathbf{A}_{ij} = \mathbf{0}$. Moreover, due to (14), the diagonal blocks $\mathbf{A}_{ii} = \mathbf{A}_i$, $i = 1, \dots, N$, and $\mathbf{A}_{ij} = \mathbf{R}_i \mathbf{A} \mathbf{R}_j^\top$, $i, j = 1, \dots, N$.

First, we solve (13) iteratively by the one-level additive Schwarz method which is (in the DG context) equivalent to the block Jacobi method. Let $\mathbf{u}^\ell = (\mathbf{u}_1^\ell, \dots, \mathbf{u}_N^\ell)^\top$ denote the ℓ -th approximation of \mathbf{u} , then we have

$$\mathbf{A}_i \mathbf{u}_i^{\ell+1} = \mathbf{g}_i - \sum_{j=1, j \neq i}^N \mathbf{A}_{ij} \mathbf{u}_j^\ell, \quad i = 1, \dots, N, \quad \ell = 0, 1, 2, \dots \quad (18)$$

In virtue of (16), scheme (18) is equivalent to

$$\mathbf{u}^{\ell+1} = \mathbf{u}^\ell + \mathbf{N}_{\text{add},1}^{-1} (\mathbf{g} - \mathbf{A} \mathbf{u}^\ell), \quad \ell = 0, 1, 2, \dots \quad (19)$$

Additionally, the two-level method read: For $\ell = 1, 2, \dots$, set

$$\text{step (i)} \quad \mathbf{u}^{\ell+1/2} := \mathbf{u}^\ell + \mathbf{N}_{\text{add},1}^{-1} (\mathbf{g} - \mathbf{A} \mathbf{u}^\ell), \quad (20a)$$

$$\text{step (ii)} \quad \mathbf{u}^{\ell+1} := \mathbf{u}^{\ell+1/2} + \mathbf{R}_0^\top \mathbf{A}_0^{-1} \mathbf{R}_0 (\mathbf{g} - \mathbf{A} \mathbf{u}^{\ell+1/2}), \quad (20b)$$

which means that the residual of the approximate solution computed locally on fine meshes is restricted to the coarse global mesh, the coarse problem is solved, and the ‘‘coarse’’ residual is projected back to the fine mesh to update the solution.

Let us consider a modification of (20b) in the form

$$\text{step (ii')} \quad \mathbf{u}^{\ell+1} := \mathbf{u}^{\ell+1/2} + \mathbf{R}_0^\top \mathbf{A}_0^{-1} \mathbf{R}_0 (\mathbf{g} - \mathbf{A} \mathbf{u}^\ell), \quad (21)$$

which can be executed independently of step (i). However, it does not converge in general but can be used as a preconditioner, cf. Section 3.3.1. In the following, we discuss both variants (ii) and (ii').

3.3.1 Variant (ii')

Inserting (20a) into (21) and using (15)–(16) gives

$$\begin{aligned} \mathbf{u}^{\ell+1} &= \mathbf{u}^\ell + \mathbf{N}_{\text{add},1}^{-1} (\mathbf{g} - \mathbf{A} \mathbf{u}^\ell) + \mathbf{R}_0^\top \mathbf{A}_0^{-1} \mathbf{R}_0 (\mathbf{g} - \mathbf{A} \mathbf{u}^\ell) \\ &= \mathbf{u}^\ell + \mathbf{N}_{\text{add},2}^{-1} (\mathbf{g} - \mathbf{A} \mathbf{u}^\ell), \quad \ell = 0, 1, \dots \end{aligned} \quad (22)$$

If $\mathbf{u}^\ell \rightarrow \mathbf{u}$ for $\ell \rightarrow \infty$, then the limit \mathbf{u} is also the solution of (13). Moreover, with respect to (22), the vector \mathbf{u} fulfills

$$\mathbf{P}_{\text{add},2} \mathbf{u} = \mathbf{N}_{\text{add},2}^{-1} \mathbf{A} \mathbf{u} = \mathbf{N}_{\text{add},2}^{-1} \mathbf{g}. \quad (23)$$

Therefore, the two-level additive Schwarz preconditioner (15) corresponds to the iterative method (20a) & (21).

3.3.2 Variant (ii)

Similarly as in Section 3.3.1, inserting (20a) into (20b) and using (15)–(16), we get

$$\begin{aligned} \mathbf{u}^{\ell+1} &= \mathbf{u}^\ell + \mathbf{N}_{\text{add},1}^{-1} (\mathbf{g} - \mathbf{A} \mathbf{u}^\ell) + \mathbf{R}_0^\top \mathbf{A}_0^{-1} \mathbf{R}_0 \left(\mathbf{g} - \mathbf{A} (\mathbf{u}^\ell + \mathbf{N}_{\text{add},1}^{-1} (\mathbf{g} - \mathbf{A} \mathbf{u}^\ell)) \right) \\ &= \mathbf{u}^\ell + \left(\mathbf{N}_{\text{add},1}^{-1} + \mathbf{R}_0^\top \mathbf{A}_0^{-1} \mathbf{R}_0 - \mathbf{R}_0^\top \mathbf{A}_0^{-1} \mathbf{R}_0 \mathbf{A} \mathbf{N}_{\text{add},1}^{-1} \right) (\mathbf{g} - \mathbf{A} \mathbf{u}^\ell). \end{aligned} \quad (24)$$

Therefore, using the same argumentation as in (23), the preconditioner corresponding to the iterative method (20a) & (20b) reads

$$\begin{aligned} \mathbf{N}_{\text{hyb}}^{-1} &:= \mathbf{N}_{\text{add},1}^{-1} + \mathbf{R}_0^\top \mathbf{A}_0^{-1} \mathbf{R}_0 - \mathbf{R}_0^\top \mathbf{A}_0^{-1} \mathbf{R}_0 \mathbf{A} \mathbf{N}_{\text{add},1}^{-1} \\ &= \sum_{i=1}^N \mathbf{R}_i^\top \mathbf{A}_i^{-1} \mathbf{R}_i + \mathbf{R}_0^\top \mathbf{A}_0^{-1} \mathbf{R}_0 \left(\mathbf{I} - \mathbf{A} \sum_{i=1}^N \mathbf{R}_i^\top \mathbf{A}_i^{-1} \mathbf{R}_i \right). \end{aligned} \quad (25)$$

Due to (14)–(16), the preconditioner operator has the form

$$\begin{aligned} \mathbf{P}_{\text{hyb}} &:= \mathbf{N}_{\text{hyb}}^{-1} \mathbf{A} = \mathbf{P}_{\text{add},1} + \mathbf{P}_0 - \mathbf{P}_0 \mathbf{P}_{\text{add},1} = \mathbf{I} - (\mathbf{I} - \mathbf{P}_0)(\mathbf{I} - \mathbf{P}_{\text{add},1}) \\ &= \mathbf{I} - (\mathbf{I} - \mathbf{P}_0) \left(\mathbf{I} - \sum_{i=1}^N \mathbf{P}_i \right), \end{aligned} \quad (26)$$

which is actually a *hybrid operator*, it is additive with respect to the local components and multiplicative with respect to the levels.

However, the preconditioner \mathbf{P}_{hyb} is not symmetric so it is not possible to use it in combination with, e.g. conjugate gradient method. The symmetric variant of (26) was proposed in [32] in context of conforming finite element method, see also [38, Section 2.5.2]. Therefore, we introduce a symmetric variant of (26)

$$\begin{aligned} \mathbf{P}_{\text{hyb},S} &:= \mathbf{I} - (\mathbf{I} - \mathbf{P}_0) \left(\mathbf{I} - \sum_{i=1}^N \mathbf{P}_i \right) (\mathbf{I} - \mathbf{P}_0) \\ &= \mathbf{P}_0 + (\mathbf{I} - \mathbf{P}_0) \sum_{i=1}^N \mathbf{P}_i (\mathbf{I} - \mathbf{P}_0), \end{aligned} \quad (27)$$

where last equality follows from (17). We analyze the preconditioned operator $\mathbf{P}_{\text{hyb},S}$ in Section 4. The preconditioner $\mathbf{N}_{\text{hyb},S}^{-1}$ corresponding to the preconditioner operator $\mathbf{P}_{\text{hyb},S} =: \mathbf{N}_{\text{hyb},S}^{-1} \mathbf{A}$ from (27) can be derived as

$$\mathbf{N}_{\text{hyb},S}^{-1} = \mathbf{R}_0^\top \mathbf{A}_0^{-1} \mathbf{R}_0 + (\mathbf{I} - \mathbf{R}_0^\top \mathbf{A}_0^{-1} \mathbf{R}_0 \mathbf{A}) \sum_{i=1}^N \mathbf{R}_i^\top \mathbf{A}_i^{-1} \mathbf{R}_i (\mathbf{I} - \mathbf{A} \mathbf{R}_0^\top \mathbf{A}_0^{-1} \mathbf{R}_0). \quad (28)$$

Algorithms 1 and 2 describe the applications of preconditioners $\mathbf{N}_{\text{add},2}^{-1}$ and $\mathbf{N}_{\text{hyb},S}^{-1}$ introduced in (15) and (28), respectively. Whereas Algorithm 1 allows to solve the local fine problems (with \mathbf{A}_i , $i = 1, \dots, N$) together with the global coarse problem (with \mathbf{A}_0) in parallel, Algorithm 2 requires solving the global coarse problem first, then the local fine problems, and finally the global coarse problem. Additionally, two multiplications by \mathbf{A} have to be performed. The multiplication by \mathbf{A} is typically much cheaper than solution of local or global problems. Moreover, if the global coarse problem is smaller than a local one then the application of the preconditioner $\mathbf{N}_{\text{hyb},S}^{-1}$ exhibits only a small increase of the computational time in comparison to the preconditioner $\mathbf{N}_{\text{add},2}^{-1}$.

Algorithm 1: Application of preconditioner $\mathbf{N}_{\text{add},2}^{-1}$ from (15): $\mathbf{u} \leftarrow \mathbf{N}_{\text{add},2}^{-1} \mathbf{x}$

- 1: **input** matrices \mathbf{A} , \mathbf{A}_i , \mathbf{R}_i , $i = 0, \dots, N$, vector \mathbf{x}
 - 2: $\mathbf{x}_i := \mathbf{R}_i \mathbf{x}$ and solve $\mathbf{A}_i \mathbf{y}_i = \mathbf{x}_i$ for $i = 0, \dots, N$
 - 3: **output** vector $\mathbf{u} := \sum_{i=0}^N \mathbf{R}_i^\top \mathbf{y}_i$
-

4 Numerical analysis

In this section we derive the bound of the hybrid Schwarz operator (27). For the sake of simplicity, we consider a quasi-uniform meshes \mathcal{T}_h and \mathcal{T}_H with mesh steps h and H , respectively, and constant polynomial degrees p and q . Let $H^s(\mathcal{T}_h)$ be the broken Sobolev space consisting of piecewise regular functions belonging to $H^s(K)$ for $K \in \mathcal{T}_h$, $s = 1, 2$. Moreover, we assume \mathbf{K} being

Algorithm 2: Application of preconditioner $N_{\text{hyb,S}}^{-1}$ from (28): $\mathbf{u} \leftarrow N_{\text{hyb,S}}^{-1} \mathbf{x}$

- 1: **input** matrices \mathbf{A} , \mathbf{A}_i , \mathbf{R}_i , $i = 0, \dots, N$, vector \mathbf{x}
 - 2: $\mathbf{x}_0 := \mathbf{R}_0 \mathbf{x}$ and solve $\mathbf{A}_0 \mathbf{y}_0 = \mathbf{x}_0$
 - 3: $\mathbf{z}_0 := \mathbf{R}_0^T \mathbf{y}_0$, $\mathbf{z} := \mathbf{x} - \mathbf{A} \mathbf{z}_0$
 - 4: $\mathbf{z}_i := \mathbf{R}_i \mathbf{z}$ and solve $\mathbf{A}_i \mathbf{y}_i = \mathbf{z}_i$ for $i = 1, \dots, N$
 - 5: $\mathbf{y} := \sum_{i=1}^N \mathbf{R}_i^T \mathbf{y}_i$
 - 6: $\mathbf{w}_0 := \mathbf{R}_0 \mathbf{A} \mathbf{y}$ and solve $\mathbf{A}_0 \mathbf{v}_0 = \mathbf{w}_0$
 - 7: **output** vector $\mathbf{u} = \mathbf{z}_0 + \mathbf{y} - \mathbf{R}_0^T \mathbf{v}_0$
-

constant in Ω , hence, we put $k_0 = k_1 = 1$ in (2). The notation $a \lesssim b$ means that there exists a constant C independent of discretization parameters such that $a \leq C b$.

We assume that Ω is convex, $g \in L^2(\Omega)$, and consider the dual problem

$$\begin{aligned} -\nabla \cdot (\nabla z) &= g && \text{in } \Omega, \\ z &= 0 && \text{on } \Gamma. \end{aligned} \quad (29)$$

The weak solution of (29) fulfills $z \in H^2(\Omega)$ and $\|z\|_{H^2(\Omega)} \lesssim \|g\|_{L^2(\Omega)}$. We note that the adjoint consistency of \mathcal{A}_h implies (e.g., [17, Lemma 2.48])

$$\mathcal{A}_h(\varphi, z) = (g, \varphi) \quad \forall \varphi \in H^2(\mathcal{T}_h). \quad (30)$$

4.1 Properties of \mathcal{A}_h

We use the DG-norm defined as follows

$$\|v_h\|^2 = |\nabla v_h|_{H^1(\mathcal{T}_h)}^2 + \bar{\sigma} \sum_{\gamma \in \Gamma_h} \|[[v_h]]\|_{L^2(\gamma)}^2, \quad (31)$$

where $\bar{\sigma} = p^2/h$. The form \mathcal{A}_h from (6) is coercive and continuous, namely

$$\|u_h\|^2 \lesssim \mathcal{A}_h(u_h, u_h), \quad u_h \in S_h, \quad (32)$$

$$|\mathcal{A}_h(u_h, v_h)| \lesssim \|u_h\| \|v_h\|, \quad u_h, v_h \in S_h, \quad (33)$$

$$|\mathcal{A}_h(u_h, v)| \lesssim \|u_h\| \|v\|_\sigma, \quad u \in S_h, v \in H^2(\mathcal{T}_h), \quad (34)$$

where $\|u\|_\sigma^2 := \|u\|^2 + (\bar{\sigma})^{-1} \sum_{\gamma \in \Gamma_h} \|\langle \nabla u \rangle \cdot \mathbf{n}_\gamma\|_{L^2(\gamma)}^2$. Finally, we use the following interpolation estimates following, e.g. from [7, Section 2] or [11, Section 3.3]: let $z \in H^2(\mathcal{K})$, $\mathcal{K} \in \mathcal{T}_H$ and $\Pi_0 z$ be its piece-wise polynomial interpolation in $S_{h,0}$ then

$$\|z - \Pi_0 z\|_{H^r(\mathcal{K})} \lesssim \frac{H^{2-r}}{q^{2-r}} \|z\|_{H^2(\mathcal{K})}, \quad r = 0, 1, \quad (35)$$

$$\|D^\alpha(z - \Pi_0 z)\|_{L^2(\partial\mathcal{K})} \lesssim \frac{H^{2-|\alpha|-1/2}}{q^{2-|\alpha|-1/2}} \|z\|_{H^2(\mathcal{K})}, \quad 0 \leq |\alpha| \leq 1,$$

where α is a multi-index of length $|\alpha|$. Using estimates (35), we can derive

$$\|z - \Pi_0 z\|_\sigma \lesssim \frac{H}{q} \|z\|_{H^2(\Omega)}, \quad z \in H^2(\Omega). \quad (36)$$

4.2 Auxiliary results

For any $w_h \in S_h$, we define its projection $w_H := P_0 w_h = R_0^T \tilde{P}_0 w_h$, where operators R_0^T , \tilde{P}_0 and P_0 are given by (11). Therefore, using (10) – (11), we have the Galerkin orthogonality

$$\mathcal{A}_h(w_h - w_H, R_0^T v_0) = 0 \quad \forall v_0 \in S_{h,0}. \quad (37)$$

Lemma 4.1. *Let $w_h \in S_h$ and $w_H \in S_{h,0}$ be its projection satisfying (37). Then*

$$\|w_h - w_H\| \lesssim \|w_h\|, \quad \|w_h - w_H\|_{L^2(\Omega)} \lesssim \frac{H}{q} \|w_h\|. \quad (38)$$

Proof. Using the coercivity and boundedness (33)–(32) and (37), we have

$$\|w_h - w_H\|^2 \lesssim \mathcal{A}_h(w_h - w_H, w_h - w_H) = \mathcal{A}_h(w_h - w_H, w_h) \lesssim \|w_h - w_H\| \|w_h\|,$$

which proves first inequality in (38).

To prove the second, we consider the dual problem (29) with $g := w_h - w_H$. Putting $\varphi := w_h - w_H$ in (30), using (37) and (34), we have

$$\begin{aligned} \|w_h - w_H\|_{L^2(\Omega)}^2 &= \mathcal{A}_h(w_h - w_H, z) = \mathcal{A}_h(w_h - w_H, z - \Pi_0 z) \\ &\lesssim \|w_h - w_H\| \|z - \Pi_0 z\|_\sigma, \end{aligned} \quad (39)$$

where $\Pi_0 z$ is the projection of z in $S_{h,0}$. The approximation bound (36), the first estimate in (38) and the bound of $\|z\|_{H^2(\Omega)}$ gives the second estimate in (38). \square

Lemma 4.2. *Let $u_h \in S_h$ and $u_h \in \text{Range}(I - P_0)$. Then $u_h - P_0 u_h = u_h$ and*

$$\|u_h\|_{L^2(\Omega)} \lesssim \frac{H}{q} \|u_h\|. \quad (40)$$

Proof. As $u_h \in \text{Range}(I - P_0)$, then $u_h = w_h - P_0 w_h$ for some $w_h \in S_h$. Hence,

$$u_h - P_0 u_h = (w_h - P_0 w_h) - P_0(w_h - P_0 w_h) = w_h - P_0 w_h = u_h$$

since $P_0^2 = P_0$, cf. (17). Moreover, estimate (40) follows directly from (38). \square

Finally, we employ the following auxiliary lemmas.

Lemma 4.3 ([6], Lemma 4.2). *Let $u \in S_h$ such that it has a unique decomposition $u = \sum_{i=1}^N R_i^\top u_i$ with $u_i \in S_{h,i}$. Then*

$$\left| \sum_{i,j=1, i \neq j}^N \mathcal{A}_h(R_i^\top u_i, R_j^\top u_j) \right| \lesssim \left(\|u\|^2 + \bar{\sigma} \sum_{\mathcal{K} \in \mathcal{T}_H} \|u\|_{L^2(\partial \mathcal{K})}^2 \right). \quad (41)$$

Lemma 4.4. *For any $v_h \in S_h$, we have the following inequality*

$$\sum_{\mathcal{K} \in \mathcal{T}_H} \|v_h\|_{L^2(\partial \mathcal{K})}^2 \lesssim \|v_h\| \|v_h\|_{L^2(\Omega)} + \frac{1}{H} \|v_h\|_{L^2(\Omega)}^2, \quad v_h \in S_h. \quad (42)$$

Proof. The proof is a direct consequence of [37, Lemma 5]. \square

4.3 Main theoretical results

We derive a bound of the preconditioned operator using the approach from [38]. The following three assumptions are required.

Assumption 4.5. (*Local stability*) *There exists a constant ω , $0 \leq \omega \leq 2$, such that*

$$\mathcal{A}_h(R_i^\top u_i, R_i^\top u_i) \leq \omega \mathcal{A}_{h,i}(u_i, u_i) \quad \forall u_i \in S_{h,i}, \quad i = 0, \dots, N.$$

Assumption 4.6. (*Strengthened Cauchy-Schwarz inequalities*) *There exist constants $0 \leq \varepsilon_{ij} \leq 1$, $i, j = 1, \dots, N$, such that*

$$|\mathcal{A}_h(R_i^\top u_i, R_j^\top u_j)| \leq \varepsilon_{ij} \mathcal{A}_h(R_i^\top u_i, R_i^\top u_i)^{1/2} \mathcal{A}_h(R_j^\top u_j, R_j^\top u_j)^{1/2}, \quad i, j = 1, \dots, N,$$

for all $u_i \in S_{h,i}$, $u_j \in S_{h,j}$. By $\rho(\varepsilon)$ we denote the spectral radius of $\varepsilon = \{\varepsilon_{ij}\}_{i,j=1}^N$.

Assumption 4.7. (Stable decomposition) *There exists a constant C_0^2 , such that any $u \in \text{Range}(I - P_0)$ admits the decomposition $u = \sum_{i=1}^N R_i^\top u_i$, $u_i \in S_{h,i}$ that satisfies*

$$\sum_{i=1}^N \mathcal{A}_{h,i}(u_i, u_i) \leq C_0^2 \mathcal{A}_h(u, u). \quad (43)$$

The condition number bound of hybrid Schwarz preconditioner is the following.

Theorem 4.8. [38, Theorem 2.13] *Let Assumptions 4.5–4.7 be satisfied. Then the condition number of the hybrid preconditioned operator (27) satisfies*

$$\kappa(\mathbf{P}_{\text{hyb,S}}) \leq \max\{1, C_0^2\} \max\{1, \omega \rho(\varepsilon)\}, \quad (44)$$

where C_0^2 , $\rho(\varepsilon)$ and ω are constants from (4.7), (4.6) and (4.5), respectively.

Assumption 4.5 is valid due to (10) with equality for $\omega = 1$. Since \mathcal{A}_h is symmetric and coercive, the inequality in Assumption 4.6 gives $\epsilon_{ij} = 1$ if $i = j$ or Ω_i and Ω_j are neighboring. Otherwise, $\epsilon_{ij} = 0$. Then Assumption 4.6 is valid with $\rho(\varepsilon) = N_S + 1$, where N_S is the maximum number of adjacent subdomains to any given subdomain in the domain decomposition. Finally, we prove the last assumption.

Lemma 4.9. *The estimate (43) is fulfilled with the constant*

$$C_0^2 = C_\sigma \frac{H p^2}{h q}, \quad (45)$$

where $C_\sigma > 0$ is independent of the mesh sizes h , H and the polynomial degrees p , q .

Proof. Let $u \in \text{Range}(I - P_0)$ with the unique decomposition $u = \sum_{i=1}^N R_i^\top u_i$. Hence, we can write the following identity

$$\mathcal{A}_h(u, u) = \sum_{i=1}^N \mathcal{A}_{h,i}(u_i, u_i) + \sum_{i,j=1, i \neq j}^N \mathcal{A}_h(R_i^\top u_i, R_j^\top u_j). \quad (46)$$

The triangle inequality gives

$$\left| \sum_{i=1}^N \mathcal{A}_{h,i}(u_i, u_i) \right| \leq |\mathcal{A}_h(u, u)| + \left| \sum_{i,j=1, i \neq j}^N \mathcal{A}_h(R_i^\top u_i, R_j^\top u_j) \right|. \quad (47)$$

We bound the last term in (47) by Lemma 4.3 and get

$$\left| \sum_{i=1}^N \mathcal{A}_{h,i}(u_i, u_i) \right| \lesssim |\mathcal{A}_h(u, u)| + \left(\|u\|^2 + \bar{\sigma} \sum_{\mathcal{K} \in \mathcal{T}_H} \|u\|_{L^2(\partial \mathcal{K})}^2 \right). \quad (48)$$

Moreover, using (32), (40), and (42), we have

$$\|u\|^2 + \bar{\sigma} \sum_{\mathcal{K} \in \mathcal{T}_H} \|u\|_{L^2(\partial \mathcal{K})}^2 \lesssim \left(1 + \bar{\sigma} \frac{H}{q} + \bar{\sigma} \frac{H^2}{Hq} \right) \|u\|^2 \lesssim \frac{p^2 H}{h q} \mathcal{A}_h(u, u),$$

which together with (48) proves (45). \square

Corollary 4.10. *Theorem 4.8 and Lemma 4.9 implies that the condition number of the hybrid Schwarz operator (27) satisfies*

$$\kappa(\mathbf{P}_{\text{hyb,S}}) \lesssim \frac{H p^2}{h q} (N_S + 1), \quad (49)$$

where h , p , H , q are the discretization parameters and N_S is the maximum number of neighboring subdomains.

Remark 1. The spectral bound of the additive Schwarz operator (15) is (cf. [7])

$$\kappa(\mathbf{P}_{\text{add},2}) \lesssim \frac{H}{h} \frac{p^2}{q} (N_S + 2). \quad (50)$$

In practice, the constant N_S is usually between 7 and 12. Hence, the bound (49) of the hybrid preconditioner is only slightly better than bound (50) of the additive one. They are the same in terms of h , H , p , and q .

4.4 Computational costs

Finally, we discuss the computational costs of an iterative solver employing the presented preconditioners. The most expensive part of Algorithms 1–2 is the performance of the preconditioner, which exhibits the solution of the local (fine) systems and the global (coarse) one

$$\mathbf{A}_i \mathbf{y}_i = \mathbf{x}_i, \quad i = 1, \dots, N, \quad \text{and} \quad \mathbf{A}_0 \mathbf{y}_0 = \mathbf{x}_0, \quad (51)$$

respectively. These systems are usually solved by a direct method, e.g., MUMPS library [33, 1, 2]. For simplicity, we neglect the other parts of the computation, such as applications of the prolongation and restrictions operators or the multiplication of a vector by the (total) matrix \mathbf{A} which is executed in iterative solvers. Moreover, we assume that we have enough computer cores and that each algebraic system from (51) is solved by one core so that all independent algebraic systems can be solved in parallel. We measure computational costs by

- (i) **flops** – the maximum of the number of *floating point operations* per one core,
- (ii) **com** – the number of *communication operations* between a core and other ones.

4.4.1 Floating point operations

The solution of each linear algebraic system from (51) by MUMPS has two steps:

- (1) the *factorization* of the system, which is carried out using $\text{fl}_{\text{fac}}(n)$ floating point operations, where n denotes the size of the system,
- (2) the *assembling* of the solution using $\text{fl}_{\text{ass}}(n)$ floating point operations.

The factorization is performed only once before the start of the iterative solver, whereas the assembling is performed at each solver iteration. Both values fl_{fac} and fl_{ass} are provided by MUMPS.

We estimate the maximum of the number of floating-point operations per one core of the iterative solver. Let $n_i := \dim S_{h,i}$, $i = 1, \dots, N$ denote the dimension of the local spaces (8) and similarly $n_0 := \dim S_{h,0}$, cf. (9). The *factorization* of matrices $\mathbf{A}_i \in \mathbb{R}^{n_i \times n_i}$ can be carried out independently for each $i = 0, \dots, N$, so the maximum of the number of floating point operations per core is

$$\text{Fl}_{\text{fac}} := \max_{i=0, \dots, N} \text{fl}_{\text{fac}}(n_i). \quad (52)$$

The *assembling* of the solutions of the local systems and the global coarse one can be executed in parallel only for the additive preconditioner $\mathbf{N}_{\text{add},2}^{-1}$. For the hybrid preconditioner $\mathbf{N}_{\text{hyb},S}^{-1}$, we solve the local systems in parallel and (twice) the global system sequentially. Hence, the corresponding maximum of the number of floating point operations per core for assembling is

$$\text{Fl}_{\text{ass}} := \begin{cases} \max_{i=0, \dots, N} \text{fl}_{\text{ass}}(n_i) & \text{for } \mathbf{N}_{\text{add},2}^{-1}, \\ \max_{i=1, \dots, N} \text{fl}_{\text{ass}}(n_i) + 2\text{fl}_{\text{ass}}(n_0) & \text{for } \mathbf{N}_{\text{hyb},S}^{-1}, \end{cases} \quad (53)$$

at each solver iteration. Let iter denote the number of iterations of the iterative solver then, using (52)–(53), the maximum of the number of floating point operations per one core is

$$\text{flops} := \text{Fl}_{\text{fac}} + \text{iter} \text{Fl}_{\text{ass}}. \quad (54)$$

4.5 Communication operations

We are aware that the following considerations exhibit a significant simplification and that the number of the communication operations strongly depends on the implementation. We assume that all vectors appearing in the computations are stored in copies at each computer core and that each matrix \mathbf{A}_i , $i = 0, \dots, N$ is allocated only at one processor. However, for the hybrid operator case, we assume that the “coarse” matrix \mathbf{A}_0 is stored in copies at each core. This causes a (small) increase of the memory requirements, but the same coarse global problem can be solved at each core, which keeps the maximum of the floating point operations whereas reduces the communication among the cores.

Therefore, all communication operators among the cores are given by the distribution of the solution of local problems, i.e., the vectors of size approximately n/N , n is the size of \mathbf{A} and N is number of cores. Hence, each core communicates with the other $N - 1$ cores and then the number of *communication operations* per one core can be estimated by

$$\text{com} = \text{iter } n (N - 1)/N, \quad (55)$$

where *iter* is the number of iterations of the iterative solver.

We remind that both (54) and (55) have only an informative character since some parts of the iterative solvers (multiplication by \mathbf{A} , application of \mathbf{R}_i , \mathbf{R}_i^T) are not considered. Nevertheless, they provide additional information related to the computational costs.

5 Numerical examples

In this section, we present the numerical study of the convergence of the preconditioners presented in Section 3. The aim is to show

- the *weak scalability* of the iterative methods, i.e., the computational costs are ideally constant for a fixed ratio between the size of the problem and the number of computer cores,
- the comparison of efficiency of the additive and hybrid Schwarz preconditioners.

Therefore, we performed computations using a sequence of (quasi) uniform meshes with increasing numbers of elements $\#\mathcal{T}_h$ and the number of subdomains N is chosen such that the number of elements within each Ω_i , $i = 1, \dots, N$ is (approximately constant). Namely we keep the ratio $\#\mathcal{T}_h/N \approx 100$ and $\#\mathcal{T}_h/N \approx 1000$. The coarse mesh \mathcal{T}_H is chosen such that each \mathcal{K} is just one subdomain Ω_i , $i = 1, \dots, N$ or each Ω_i is divided into several \mathcal{K} .

Linear systems (13) are solved using the conjugate gradient (CG) method with the preconditioners $\mathbf{N}_{\text{add},2}^{-1}$ and $\mathbf{N}_{\text{hyb},S}^{-1}$ given by (15) and (28), respectively. The CG algorithm is stopped when the relative preconditioned residual r_{rel} fulfills

$$r_{\text{rel}}^\ell := \|\mathbf{N}^{-1}(\mathbf{A}\mathbf{u}^\ell - \mathbf{g})\| / \|\mathbf{N}^{-1}(\mathbf{A}\mathbf{u}^0 - \mathbf{g})\| \leq \omega, \quad (56)$$

where \mathbf{N}^{-1} denotes a preconditioner and $\omega > 0$ is the prescribed user tolerance. We employ P_p , $p = 1, 2, 3$ polynomial approximations for each case.

5.1 Laplace problem

First, we consider a simple toy example

$$-\Delta u = -2x_1(1 - x_1) - 2x_2(1 - x_2) \quad \text{in } \Omega = (0, 1)^2, \quad (57)$$

with the homogeneous Dirichlet boundary condition on Γ which gives the exact solution $u = x_1(1 - x_1)x_2(1 - x_2)$. The initial approximation \mathbf{u}^0 corresponds to a highly oscillating function (namely $u = \sum_{i,j=1}^3 \sin(2\pi i x_1) \sin(2\pi j x_2)$) in order to avoid a possible superconvergence due to the presence of particular frequency modes, cf. [22]. We set $\omega = 10^{-12}$ in (56).

The results achieved are given in Tables 1–3, where we present

- $\#\mathcal{T}_h$ – the number of elements of the fine mesh,
- N – the number of subdomains Ω_i generated by METIS [29],
- $\#\mathcal{T}_{h,i} := \#\mathcal{T}_h/N$ – the average number of elements in Ω_i , $i = 1, \dots, N$,
- $\#\mathcal{T}_H$ – the number of elements of the coarse mesh,
- **iter** – the number of (preconditioned) CG iterations necessary to achieve (56),
- **Mflops** – the number of floating point operations given by (54), $\text{Mflops} = 10^6 \text{flops}$,
- **Mcom** – the number of communication operations given by (55), $\text{Mcom} = 10^6 \text{com}$.

Table 1 shows the results corresponding to $\#\mathcal{T}_h/N = \#\mathcal{T}_{h,i} \approx 100$ and each subdomain Ω_i , $i = 1, \dots, N$ is just one element $\mathcal{K} \in \mathcal{T}_H$. Furthermore, Table 2 contains the results with $\#\mathcal{T}_h/N = \#\mathcal{T}_{h,i} \approx 1000$ and each subdomain Ω_i consists of 1, 5, and 10 coarse elements $\mathcal{K} \in \mathcal{T}_H$.

Moreover, Table 3 presents the results for the finest mesh \mathcal{T}_h having 32768 elements, the number of sub-domains is $N = 8, 16, 32, 64$, and the number of elements of the coarse mesh is fixed to 128 (however, the coarse meshes are not the same due to kind of construction). Finally, Figure 1 shows the convergence of the CG method for the setting from Table 1, namely the dependence of r_{rel}^ℓ with respect to $\ell = 0, 1, \dots$, cf. (56). We observe the following.

- Tables 1–2: For each particular p and particular preconditioner, the number of CG iterations is almost constant for increasing $\#\mathcal{T}_h$, which implies the weak scalability of both preconditioners provided that the computational costs of the coarse solver are neglected. This is not the case for the finer meshes in Table 1 where $\#\mathcal{T}_H > \#\mathcal{T}_{h,i}$ and thus the number of **flops** increases for the increasing size of the problem. However, the results of Table 2, when $\#\mathcal{T}_H \ll \#\mathcal{T}_{h,i}$, support the scalability in terms of **flops**.
- Table 3: When $\#\mathcal{T}_H$ and $\#\mathcal{T}_{h,i}$ are fixed (i.e., h and H are fixed too), we observe a slight increase in the number of **iter** for an increasing number of subdomains N . Consequently, the number of **flops** is reducing by factor at least two since the parallelism can be employed more effectively. On the other hand, the number of communication operations **com** is slightly increasing. So, the optimal choice of the number of subdomains is open and it will be the subject of further research.
- Tables 1–3: the performance of the hybrid preconditioner $\mathbf{N}_{\text{hyb},S}^{-1}$ saves about 25 – 30% of the CG iterations compared to the additive preconditioner $\mathbf{N}_{\text{add},2}^{-1}$. The value 25 – 30% also exhibits a potential benefit in computational time if the computational costs of the coarse solver are negligible (e.g., $N \ll \#\mathcal{T}_h/N$).
- Figure 1: All graphs showing the convergence of the residual with respect to the number of CG iterations support the scalability of the methods. Moreover, for the P_2 and P_3 approximation, we observe that the tolerance level $\omega = 10^{-6}$ in (56) is achieved using the smaller number of CG iterations for the increasing size of the problem.

5.2 Alternator (linearized)

This example exhibits a linearized variant of the magnetic state in the cross-section of an alternator from Section 5.3, which originates from [26]. The computational domain Ω (one quarter of the alternator) consists of the stator (Ω_s) and the rotor (Ω_r) with a gap filled by air (Ω_a); see Figure 2, left, where the geometry of the domain is shown. We consider problem (3a) with $f = 5 \cdot 10^4$ and $\mathbf{K} = \nu(x)\mathbf{I}$ such that

$$\nu(x) = \begin{cases} \mu_0^{-1} & \text{for } x \in \Omega_a, \\ \mu_1^{-1} & \text{for } x \in \Omega_s \cup \Omega_r, \end{cases} \quad (58)$$

where $\mu_0 = 1.256 \cdot 10^{-6}$, $\mu_1 = \zeta\mu_0$, $\zeta > 1$. Particularly, we use the values $\zeta = 100$ and $\zeta = 10000$. We prescribe $\nabla u \cdot \mathbf{n} = 0$ on $\Gamma_N := (0, 1) \times \{0\} \cup \{0\} \times (0, 1)$ and $u = 0$ on the rest of the boundary.

Figure 2, center and right, shows the two examples of the used meshes and the corresponding domain partition by METIS [29]. We note that this domain splitting is not aligned with the material interfaces. Usually, it is not the optimal strategy, but the presented experiments indicate a robustness of the algorithm with respect to the domain splitting. In the same way as in Section 5.1,

Table 1: Laplace problem (57), convergence of CG method with preconditioners $N_{\text{add},2}^{-1}$ and $N_{\text{hyb},S}^{-1}$, the subdomains splitting $\#\mathcal{T}_h/N \approx 100$.

additive $N_{\text{add},2}^{-1}$				$p = 1$			$p = 2$			$p = 3$		
$\#\mathcal{T}_h$	N	$\#\mathcal{T}_{h,i}$	$\#\mathcal{T}_H$	iter	Mflops	Mcom	iter	Mflops	Mcom	iter	Mflops	Mcom
1152	11	104	11	78	0.8	0.2	123	5.5	0.8	150	19.7	1.6
2048	20	102	20	85	0.9	0.5	128	5.7	1.5	155	20.0	3.0
4608	46	100	46	93	0.9	1.3	140	5.8	3.8	161	20.1	7.3
8192	81	101	81	101	1.1	2.5	143	6.5	6.9	168	23.5	13.6
18432	184	100	184	103	4.0	5.7	137	23.2	15.1	155	82.2	28.4
32768	327	100	327	106	9.4	10.4	140	57.2	27.4	160	205.9	52.3

hybrid $N_{\text{hyb},S}^{-1}$				$p = 1$			$p = 2$			$p = 3$		
$\#\mathcal{T}_h$	N	$\#\mathcal{T}_{h,i}$	$\#\mathcal{T}_H$	iter	Mflops	Mcom	iter	Mflops	Mcom	iter	Mflops	Mcom
1152	11	104	11	58	0.7	0.2	93	4.8	0.6	112	17.1	1.2
2048	20	102	20	62	0.8	0.4	96	5.4	1.1	115	19.1	2.2
4608	46	100	46	68	1.2	0.9	97	7.2	2.6	116	25.3	5.2
8192	81	101	81	71	2.1	1.7	104	12.4	5.0	121	43.2	9.8
18432	184	100	184	70	5.7	3.8	98	34.1	10.8	112	117.3	20.5
32768	327	100	327	71	12.6	7.0	98	77.0	19.2	113	270.6	36.9

Table 2: Laplace problem (57), convergence of CG method with preconditioners $N_{\text{add},2}^{-1}$ and $N_{\text{hyb},S}^{-1}$, the subdomains splitting $\#\mathcal{T}_h/N \approx 1000$.

additive $N_{\text{add},2}^{-1}$				$p = 1$			$p = 2$			$p = 3$		
$\#\mathcal{T}_h$	N	$\#\mathcal{T}_{h,i}$	$\#\mathcal{T}_H$	iter	Mflops	Mcom	iter	Mflops	Mcom	iter	Mflops	Mcom
8192	8	1024	8	123	34.8	2.6	192	239.9	8.3	243	903.3	17.4
18432	18	1024	18	158	42.8	8.3	227	282.7	23.7	273	1011.9	47.5
32768	32	1024	32	166	48.8	15.8	239	290.8	45.5	277	1027.4	87.9

hybrid $N_{\text{hyb},S}^{-1}$				$p = 1$			$p = 2$			$p = 3$		
$\#\mathcal{T}_h$	N	$\#\mathcal{T}_{h,i}$	$\#\mathcal{T}_H$	iter	Mflops	Mcom	iter	Mflops	Mcom	iter	Mflops	Mcom
8192	8	1024	40	92	28.6	2.0	135	198.4	5.8	161	723.5	11.5
18432	18	1024	90	96	29.3	5.0	142	202.4	14.8	168	783.5	29.2
32768	32	1024	160	97	31.8	9.2	140	198.2	26.7	163	731.1	51.7

hybrid $N_{\text{hyb},S}^{-1}$				$p = 1$			$p = 2$			$p = 3$		
$\#\mathcal{T}_h$	N	$\#\mathcal{T}_{h,i}$	$\#\mathcal{T}_H$	iter	Mflops	Mcom	iter	Mflops	Mcom	iter	Mflops	Mcom
8192	8	1024	80	75	24.4	1.6	112	168.6	4.8	134	652.2	9.6
18432	18	1024	180	80	26.0	4.2	118	183.8	12.3	139	686.3	24.2
32768	32	1024	320	81	27.7	7.7	116	174.8	22.1	136	671.8	43.2

hybrid $N_{\text{hyb},S}^{-1}$				$p = 1$			$p = 2$			$p = 3$		
$\#\mathcal{T}_h$	N	$\#\mathcal{T}_{h,i}$	$\#\mathcal{T}_H$	iter	Mflops	Mcom	iter	Mflops	Mcom	iter	Mflops	Mcom
8192	8	1024	40	66	23.4	1.4	99	167.8	4.3	122	635.8	8.7
18432	18	1024	90	70	25.2	3.7	105	177.6	11.0	125	698.0	21.8
32768	32	1024	160	70	29.3	6.7	103	184.4	19.6	117	679.3	37.1

hybrid $N_{\text{hyb},S}^{-1}$				$p = 1$			$p = 2$			$p = 3$		
$\#\mathcal{T}_h$	N	$\#\mathcal{T}_{h,i}$	$\#\mathcal{T}_H$	iter	Mflops	Mcom	iter	Mflops	Mcom	iter	Mflops	Mcom
8192	8	1024	80	53	20.8	1.1	82	148.9	3.5	99	589.9	7.1
18432	18	1024	180	57	24.6	3.0	86	173.8	9.0	100	652.9	17.4
32768	32	1024	320	57	29.6	5.4	82	186.5	15.6	93	697.2	29.5

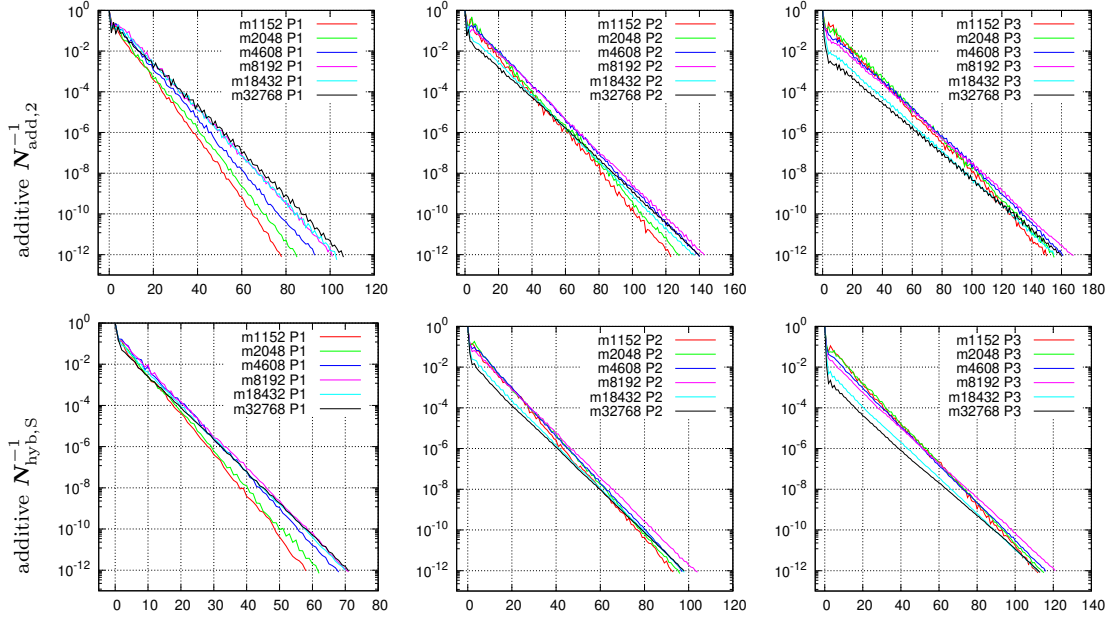


Figure 1: Laplace problem (57), convergence of CG method (r_{rel}^ℓ for $\ell = 0, 1, \dots$, cf. (56)) for preconditioners $N_{\text{add},2}^{-1}$ and $N_{\text{hyb},S}^{-1}$ with the subdomains splitting $\#\mathcal{T}_h/N \approx 100$.

Table 3: Laplace problem (57), convergence of CG method with preconditioners $N_{\text{add},2}^{-1}$ and $N_{\text{hyb},S}^{-1}$ for the finest mesh using various domain decomposition.

additive $N_{\text{add},2}^{-1}$				$p = 1$			$p = 2$			$p = 3$		
$\#\mathcal{T}_h$	N	$\#\mathcal{T}_{h,i}$	$\#\mathcal{T}_H$	iter	Mflops	Mcom	iter	Mflops	Mcom	iter	Mflops	Mcom
32768	8	4096	128	96	196.1	8.3	149	1363.3	25.6	176	5457.6	50.5
32768	16	2048	128	101	81.8	9.3	147	546.7	27.1	173	2079.7	53.1
32768	32	1024	128	104	35.3	9.9	154	210.5	29.3	178	786.0	56.5
32768	64	512	128	117	12.7	11.3	164	76.3	31.7	188	300.9	60.6
hybrid $N_{\text{hyb},S}^{-1}$				$p = 1$			$p = 2$			$p = 3$		
$\#\mathcal{T}_h$	N	$\#\mathcal{T}_{h,i}$	$\#\mathcal{T}_H$	iter	Mflops	Mcom	iter	Mflops	Mcom	iter	Mflops	Mcom
32768	8	4096	128	71	167.3	6.1	110	1185.1	18.9	128	4808.0	36.7
32768	16	2048	128	75	70.4	6.9	108	475.4	19.9	128	1855.2	39.3
32768	32	1024	128	76	31.6	7.2	111	188.9	21.1	130	720.2	41.3
32768	64	512	128	84	13.3	8.1	116	76.8	22.5	137	306.7	44.2

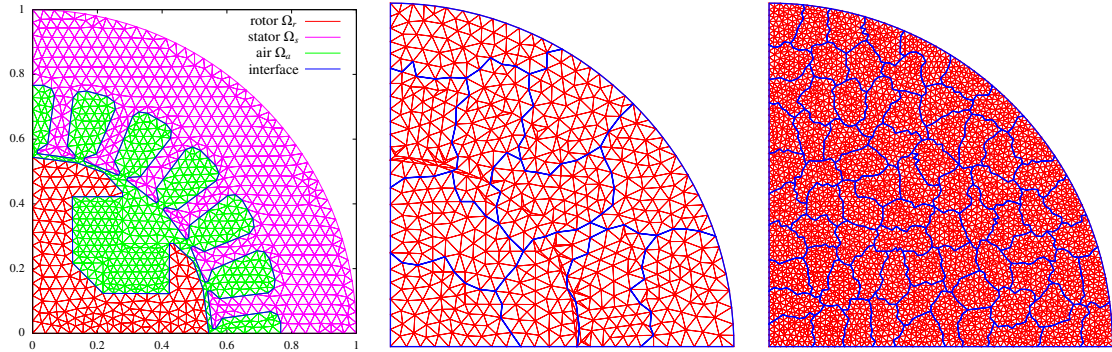


Figure 2: Linearized alternator, the computational domain Ω with its components (left) and the computational meshes \mathcal{T}_h (red) and \mathcal{T}_H (blue), with $\#\mathcal{T}_h = 1112$ & $N = \#\mathcal{T}_H = 11$ (center) and $\#\mathcal{T}_h = 7549$ & $N = \#\mathcal{T}_H = 75$ (right).

Table 4: Linearized alternator (58) with $\zeta = 100$, convergence of CG method with preconditioners $\mathbf{N}_{\text{add},2}^{-1}$ and $\mathbf{N}_{\text{hyb},S}^{-1}$ with the subdomains splitting $\#\mathcal{T}_h/N \approx 100$.

additive $\mathbf{N}_{\text{add},2}^{-1}$				$p = 1$			$p = 2$			$p = 3$		
$\#\mathcal{T}_h$	N	$\#\mathcal{T}_{h,i}$	$\#\mathcal{T}_H$	iter	Mflops	Mcom	iter	Mflops	Mcom	iter	Mflops	Mcom
1112	11	101	11	87	0.8	0.3	124	5.1	0.8	130	16.6	1.3
2025	20	101	20	110	1.2	0.6	134	6.1	1.5	154	21.4	3.0
3832	38	100	38	119	1.2	1.3	137	5.9	3.1	158	20.7	5.9
7549	75	100	75	122	1.3	2.7	154	7.0	6.9	161	23.3	12.0
14937	149	100	149	116	3.4	5.2	148	19.0	13.2	158	63.8	23.4
29819	298	100	298	133	11.0	11.9	155	58.3	27.6	153	191.1	45.5

hybrid $\mathbf{N}_{\text{hyb},S}^{-1}$				$p = 1$			$p = 2$			$p = 3$		
$\#\mathcal{T}_h$	N	$\#\mathcal{T}_{h,i}$	$\#\mathcal{T}_H$	iter	Mflops	Mcom	iter	Mflops	Mcom	iter	Mflops	Mcom
1112	11	101	11	65	0.7	0.2	94	4.4	0.6	84	13.1	0.8
2025	20	101	20	77	1.1	0.4	92	5.5	1.1	105	19.5	2.0
3832	38	100	38	80	1.4	0.9	93	7.3	2.1	99	23.5	3.7
7549	75	100	75	81	2.4	1.8	100	12.2	4.5	100	37.7	7.4
14937	149	100	149	79	5.1	3.5	95	26.6	8.5	98	84.4	14.5
29819	298	100	298	90	15.0	8.0	99	73.5	17.7	92	224.0	27.3

we present the quantities $\#\mathcal{T}_h$, $\#\mathcal{T}_{h,i}$, N and $\#\mathcal{T}_H$ together with the number of (preconditioned) CG iterations iter necessary to achieve (56) (with $\omega = 10^{-10}$), and the computational costs in Mflops and Mcom.

Tables 4 and 5 show the results for $\zeta = \mu_1/\mu_0 = 100$ in (58) for $\#\mathcal{T}_h/N \approx 100$ and $\#\mathcal{T}_h/N \approx 1000$, respectively. Moreover, Tables 6 and 7 present results corresponding to $\zeta = 10\,000$ for $\#\mathcal{T}_h/N \approx 100$ and $\#\mathcal{T}_h/N \approx 1000$, respectively.

The observations for this more complicated case are, in principle, the same as in Section 5.1. Neglecting the computational costs of the coarse solver, we have the weak scalability of the algebraic solvers, cf. Tables 5 and 7. The hybrid preconditioner $\mathbf{N}_{\text{hyb},S}^{-1}$ saves about 25 – 30% of the computational costs compared to the additive preconditioner $\mathbf{N}_{\text{add},2}^{-1}$. Similarly, the finer (coarse) mesh \mathcal{T}_H provides a more accurate approximation and reduces the number of iterations. Additionally, these observations are robust for the problem data. That is, the increase of the ratio $\zeta = k_1/k_0 = \mu_0/\mu_1$ (cf. (2) and (58)) by factor 100 leads to the increase of iter by 50 – 75% only.

5.3 Nonlinear problem with hp -mesh adaptation

Finally, we employ the presented iterative method for the numerical solution of a nonlinear elliptic problem in the combination with the anisotropic hp -mesh adaptation. Following [26, 16], the

Table 5: Linearized alternator (58) with $\zeta = 100$, convergence of CG method with preconditioners $N_{\text{add},2}^{-1}$ and $N_{\text{hyb},S}^{-1}$ with the subdomains splitting $\#\mathcal{T}_h/N \approx 1000$.

additive $N_{\text{add},2}^{-1}$				$p = 1$			$p = 2$			$p = 3$		
$\#\mathcal{T}_h$	N	$\#\mathcal{T}_{h,i}$	$\#\mathcal{T}_H$	iter	Mflops	Mcom	iter	Mflops	Mcom	iter	Mflops	Mcom
7549	7	1078	7	156	37.2	3.0	233	265.2	9.0	251	847.9	16.2
14937	14	1066	14	180	45.4	7.5	233	264.6	19.4	237	881.5	32.9
29819	29	1028	29	171	40.1	14.8	211	234.0	36.4	238	811.3	68.5

hybrid $N_{\text{hyb},S}^{-1}$				$p = 1$			$p = 2$			$p = 3$		
$\#\mathcal{T}_h$	N	$\#\mathcal{T}_{h,i}$	$\#\mathcal{T}_H$	iter	Mflops	Mcom	iter	Mflops	Mcom	iter	Mflops	Mcom
7549	7	1078	7	127	31.4	2.5	187	225.1	7.3	180	682.1	11.6
14937	14	1066	14	136	36.3	5.7	166	207.1	13.8	165	698.5	22.9
29819	29	1028	29	125	31.4	10.8	152	187.8	26.3	152	621.8	43.8

Table 6: Linearized alternator (58) with $\zeta = 10000$, convergence of CG method with preconditioners $N_{\text{add},2}^{-1}$ and $N_{\text{hyb},S}^{-1}$ with the subdomains splitting $\#\mathcal{T}_h/N \approx 100$.

additive $N_{\text{add},2}^{-1}$				$p = 1$			$p = 2$			$p = 3$		
$\#\mathcal{T}_h$	N	$\#\mathcal{T}_{h,i}$	$\#\mathcal{T}_H$	iter	Mflops	Mcom	iter	Mflops	Mcom	iter	Mflops	Mcom
1112	11	101	11	106	1.0	0.3	152	6.0	0.9	174	20.8	1.8
2025	20	101	20	131	1.3	0.8	176	7.6	2.0	223	28.6	4.3
3832	38	100	38	146	1.4	1.6	200	8.2	4.5	234	28.3	8.7
7549	75	100	75	155	1.6	3.5	231	9.7	10.3	252	32.8	18.8
14937	149	100	149	170	4.7	7.6	235	27.5	20.9	267	93.5	39.6
29819	298	100	298	190	14.9	16.9	248	83.4	44.2	269	278.0	79.9

hybrid $N_{\text{hyb},S}^{-1}$				$p = 1$			$p = 2$			$p = 3$		
$\#\mathcal{T}_h$	N	$\#\mathcal{T}_{h,i}$	$\#\mathcal{T}_H$	iter	Mflops	Mcom	iter	Mflops	Mcom	iter	Mflops	Mcom
1112	11	101	11	80	0.8	0.2	120	5.4	0.7	120	16.8	1.2
2025	20	101	20	94	1.3	0.5	132	7.4	1.5	159	26.8	3.1
3832	38	100	38	109	1.9	1.2	143	10.6	3.2	154	33.8	5.7
7549	75	100	75	112	3.2	2.5	156	18.2	7.0	156	55.3	11.6
14937	149	100	149	126	7.9	5.6	153	40.1	13.6	164	127.1	24.3
29819	298	100	298	136	21.7	12.1	161	109.2	28.7	158	329.8	47.0

Table 7: Linearized alternator (58) with $\zeta = 10000$, convergence of CG method with preconditioners $N_{\text{add},2}^{-1}$ and $N_{\text{hyb},S}^{-1}$ with the subdomains splitting $\#\mathcal{T}_h/N \approx 1000$.

additive $N_{\text{add},2}^{-1}$				$p = 1$			$p = 2$			$p = 3$		
$\#\mathcal{T}_h$	N	$\#\mathcal{T}_{h,i}$	$\#\mathcal{T}_H$	iter	Mflops	Mcom	iter	Mflops	Mcom	iter	Mflops	Mcom
7549	7	1078	7	189	43.8	3.7	287	312.5	11.1	326	1023.6	21.1
14937	14	1066	14	223	54.4	9.3	306	328.1	25.5	361	1201.0	50.1
29819	29	1028	29	219	49.6	18.9	300	307.9	51.8	344	1053.2	99.0

hybrid $N_{\text{hyb},S}^{-1}$				$p = 1$			$p = 2$			$p = 3$		
$\#\mathcal{T}_h$	N	$\#\mathcal{T}_{h,i}$	$\#\mathcal{T}_H$	iter	Mflops	Mcom	iter	Mflops	Mcom	iter	Mflops	Mcom
7549	7	1078	7	153	36.6	3.0	232	264.6	9.0	251	848.7	16.2
14937	14	1066	14	167	42.8	6.9	237	269.3	19.7	245	905.8	34.0
29819	29	1028	29	164	39.4	14.2	227	251.4	39.2	234	812.6	67.4

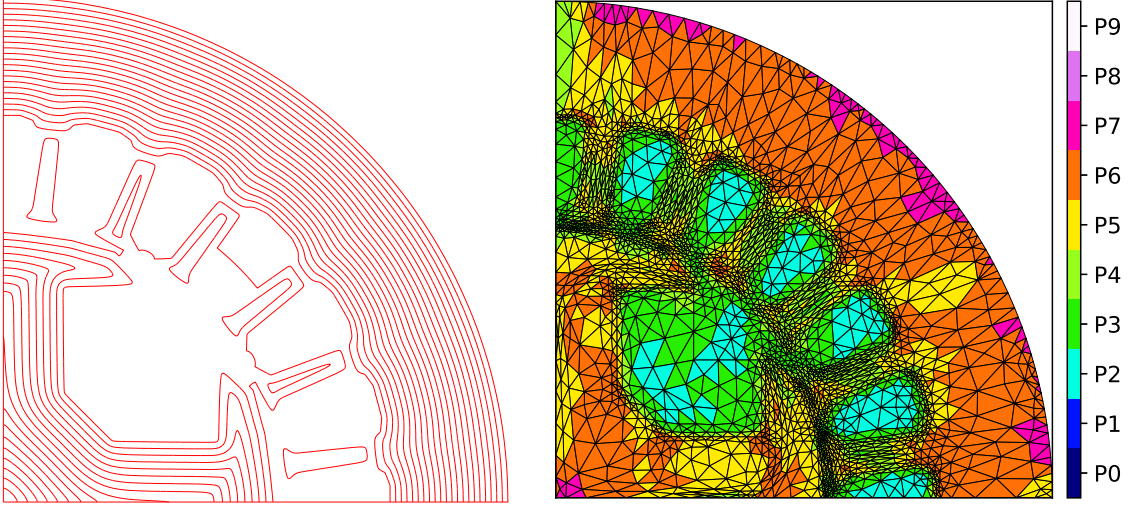


Figure 3: Nonlinear alternator (59)–(60), isolines of the solution (left) and the hp -mesh after 8 levels of mesh adaptation.

problem geometry is the same as in Figure 2 and the magnetic potential u fulfills

$$-\nabla \cdot (\nu(x, |\nabla u(x)|^2) \nabla u) = f \quad \text{in } \Omega \quad (59)$$

with

$$\nu(x, r) = \begin{cases} \frac{1}{\mu_0} & \text{for } x \in \Omega_a, \\ \frac{1}{\mu_0} \left(\alpha + (1 - \alpha) \frac{r^4}{\beta + r^4} \right) & \text{for } x \in \Omega_s \cup \Omega_r. \end{cases} \quad (60)$$

The quantity $\mu_0 = 1.256 \times 10^{-6} \text{ kg} \cdot \text{m} \cdot \text{A}^{-2} \cdot \text{s}^{-2}$ denotes the permeability of the vacuum and the material coefficients are $\alpha = 0.0003$, $\beta = 16000$ according to [26]. We consider the constant current density $f = 5 \times 10^4 \text{ A} \cdot \text{m}^{-2}$ and prescribe the mixed Dirichlet/Neumann boundary conditions as in Section 5.2. We note that these conditions differ from those in [16].

We discretize (59) again by SIPG method (cf. [16]), which leads to the similar form as (6) but \mathcal{A}_h is nonlinear in the first argument since $\mathbf{K} = \nu(x, |\nabla u(x)|^2) \mathbf{I}$ depends on u . The arising nonlinear algebraic system is solved iteratively by the Newton method where the Jacobian is evaluated by the differentiation of \mathcal{A}_h .

The iterative Newton method is stopped when the ratio between the algebraic error estimator and the discretization error estimator is below 10^{-3} , cf. [15] for details. At each Newton iteration, we solve a linear algebraic system by the conjugate gradient method with additive and/or hybrid Schwarz preconditioners, we employ the stopping criterion (56) with $\omega = 10^{-2}$. The lower value of ω leads to a small decrease in the number of Newton steps iter_N but a significant increase in the CG iterations iter_L .

Moreover, when the criterion for the Newton method is reached, we perform the re-meshing using the anisotropic hp -mesh adaptation based on the interpolation error control, we refer to [18, Chapters 5-6] for details. After the re-meshing (including the variation of polynomial approximation degrees), a new domain decomposition of Ω is employed and the computational process is repeated. We carried out eight levels of mesh refinement; at each adaptation level, Ω is divided into $N = 12$ subdomains, and the coarse mesh always has $\#\mathcal{T}_H = 48$ elements. Figure 3 shows the isolines of the solution and the final hp -mesh obtained using the hybrid preconditioner (the mesh is very similar for the additive preconditioner).

Table 8 presents the comparison of the performance of the additive and hybrid Schwarz preconditioners. For each mesh adaptation level, we show the number of mesh elements $\#\mathcal{T}_h$, number of degrees of freedom $\text{DoF} = \dim S_h$ and the accumulated number of the Newton iterations iter_N

Table 8: Nonlinear alternator (59)–(60), the convergence of the mesh adaptive algorithm.

adaptive level	additive preconditioner $N_{\text{add},2}^{-1}$				hybrid preconditioner $N_{\text{hyb},S}^{-1}$			
	$\#\mathcal{T}_h$	DoF	iter_N	iter_L	$\#\mathcal{T}_h$	DoF	iter_N	iter_L
0	2154	12 924	20	3858	2154	12 924	18	2228
1	1671	12 285	33	5564	1671	12 285	31	3618
2	1710	14 533	43	8506	1710	14 533	40	5649
3	1893	18 196	51	11 322	1893	18 196	48	8011
4	2199	23 786	60	14 717	2199	23 786	56	10 677
5	2703	33 066	69	18 092	2703	33 066	64	13 267
6	3414	47 629	80	22 378	3412	47 643	73	16 460
7	4008	63 974	91	26 909	4026	64 289	82	20 015
8	4721	86 617	105	33 056	4755	87 055	93	24 841
total		46 153	Mflops			37 398	Mflops	
costs		1268	Mcom			979	Mcom	

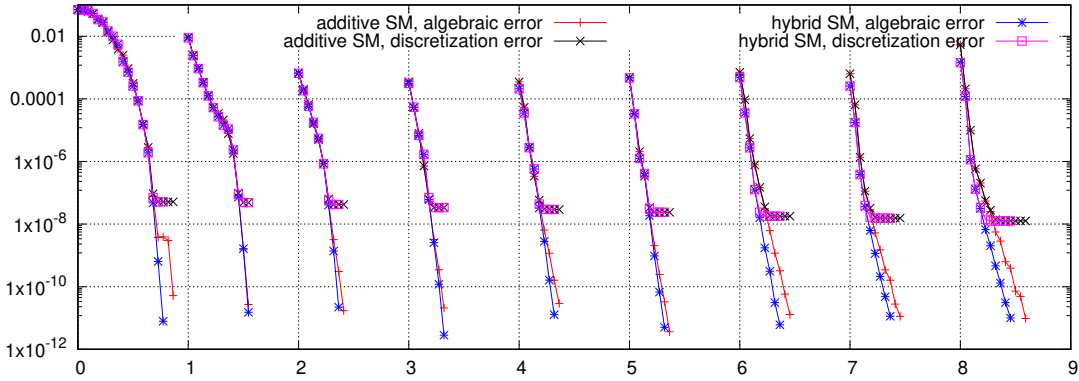


Figure 4: Nonlinear alternator (59)–(60), comparison of the convergence of the Newton method using CG solver with additive and hybrid Schwarz preconditioners.

and the CG iterations iter_L . In the last line of this table, we give the total number of Mflops and Mcom. Furthermore, Figure 4 shows the convergence of the Newton method using CG solver with additive and hybrid Schwarz preconditioners. The horizontal axes corresponds to the mesh adaptation level, each node corresponds to one Newton iteration. We plot the estimators of the algebraic and discretization errors from [15] for both preconditioners. We observe that space errors stagnate in each mesh adaptation loop at the level between 10^{-8} and 10^{-7} and the nonlinear solver stops when the ratio between the algebraic and discretization estimators is 10^{-3} . We can deduce a mild dominance of the hybrid preconditioner. However, we are aware that a rigorous comparison requires a deeper study and it will be the subject of the further research.

6 Conclusion

We presented the two-level hybrid Schwarz preconditioner for the *hp*-discontinuous Galerkin discretization of elliptic problems as an alternative to the well-established additive Schwarz approach. Whereas numerical analysis shows only a slightly better spectral bound, the numerical experiments demonstrate about 25 – 30% saving of computational costs. Moreover, the weak scalability is shown provided that the computational costs of the coarse solver are neglected. Finally, the robustness with respect to the data problem, anisotropy of the meshes and varying polynomial degree is demonstrated.

The future research will orient to more challenging problems (nonlinear, nonsymmetric, systems of equations). Additionally, the optimal choice of subdomains and coarse grid deserve a deeper

insight in order to balance the number of floating point operations and communication operations.

Acknowledgments

We are thankful to prof. Martin Gander (University of Geneva) for a fruitful discussion during his stay at the Charles University in Prague and our colleagues Michal Outrata and Petr Tichý inspiring suggestions and ideas.

References

- [1] P. R. Amestoy, A. Buttari, J.-Y. L'Excellent, and T. Mary. Performance and scalability of the block low-rank multifrontal factorization on multicore architectures. *ACM Transactions on Mathematical Software*, 45(1):2:1–2:26, 2019.
- [2] P. R. Amestoya, I. S. Duff, J. Koster, and J.-Y. L'Excellent. A fully asynchronous multifrontal solver using distributed dynamic scheduling. *SIAM J. Mat. Anal. Appl.*, 23(1):15–42, 2001.
- [3] P. Antonietti, S. Giani, and P. Houston. Domain decomposition preconditioners for discontinuous Galerkin methods for elliptic problems on complicated domains. *Journal of Scientific Computing*, 60:203–227, 2014.
- [4] Paola F. Antonietti and Blanca Ayuso. Schwarz domain decomposition preconditioners for discontinuous Galerkin approximations of elliptic problems: Non-overlapping case. *Mathematical Modelling and Numerical Analysis*, 41(1):21–54, 2007.
- [5] Paola F. Antonietti and Blanca Ayuso. Two-level Schwarz preconditioners for super penalty discontinuous Galerkin methods. *Communications in Computational Physics*, 5(2-4):398–412, 2009.
- [6] Paola F. Antonietti and Paul Houston. A class of domain decomposition preconditioners for *hp*-discontinuous Galerkin finite element methods. *J. Sci. Comput.*, 46(1):124–149, 2011.
- [7] Paola F. Antonietti, Paul Houston, and Iain Smears. A note on optimal spectral bounds for nonoverlapping domain decomposition preconditioners for *hp*-version discontinuous Galerkin methods. *International Journal of Numerical Analysis and Modeling*, 13(4):513–524, 2016.
- [8] P.F. Antonietti, P. Houston, G. Pennesi, and E. Süli. An agglomeration-based massively parallel non-overlapping additive Schwarz preconditioner for high-order discontinuous Galerkin methods on polytopic grids. *Math. Comput.*, 89(325):2047–2083, 2020.
- [9] Andrew T. Barker and Xiao-Chuan Cai. Two-level newton and hybrid Schwarz preconditioners for fluid-structure interaction. *SIAM J. Sci. Comput.*, 32(4):2395–2417, 2010.
- [10] Gabriel R. Barrenechea, Michal Bosy, Victorita Dolean, Frédéric Nataf, and Pierre-Henri Tournier. Hybrid discontinuous Galerkin discretisation and domain decomposition preconditioners for the Stokes problem. *Computational Methods in Applied Mathematics*, 19(4):703–722, 2019.
- [11] Andrea Cangiani, Zhaonan Dong, Emmanuil H. Georgoulis, and Paul Houston. *hp-Version Discontinuous Galerkin Methods on Polygonal and Polyhedral Meshes*. Springer Cham, 2017.
- [12] Claudio Canuto, Luca F. Pavarino, and Alexandre B. Pieri. BDDC preconditioners for continuous and discontinuous Galerkin methods using spectral/hp elements with variable local polynomial degree. *IMA J. Numer. Anal.*, 34(3):879–903, 2013.
- [13] D.A. Di Pietro and A. Ern. *Mathematical Aspects of Discontinuous Galerkin Methods*. Mathematiques et Applications 69. Springer Berlin Heidelberg, 2012.

- [14] Victorita Dolean, Pierre Jolivet, and Frédéric Nataf. *An Introduction to Domain Decomposition Methods Algorithms, Theory, and Parallel Implementation*. Society for Industrial and Applied Mathematics, 2015.
- [15] V. Dolejší. *hp*-DGFEM for nonlinear convection-diffusion problems. *Math. Comput. Simul.*, 87:87–118, 2013.
- [16] V. Dolejší and S. Congreve. Goal-oriented error analysis of iterative Galerkin discretizations for nonlinear problems including linearization and algebraic errors. *J. Comput. Appl. Math.*, 427:115134, 2023.
- [17] V. Dolejší and M. Feistauer. *Discontinuous Galerkin Method – Analysis and Applications to Compressible Flow*. Springer Series in Computational Mathematics 48. Springer, Cham, 2015.
- [18] V. Dolejší and G. May. *Anisotropic hp-Mesh Adaptation Methods*. Birkhäuser, 2022.
- [19] Maksymilian Dryja, Juan Galvis, and Marcus Sarkis. BDDC methods for discontinuous Galerkin discretization of elliptic problems. *Journal of Complexity*, 23(4-6):715–739, 2007.
- [20] Maksymilian Dryja and Piotr Krzyżanowski. A massively parallel nonoverlapping additive Schwarz method for discontinuous Galerkin discretization of elliptic problems. *Numer. Math.*, 132(2):347–367, 2016.
- [21] X. Feng and O. Karashian. Two-level additive Schwarz methods for a discontinuous Galerkin approximation of second order elliptic problems. *SIAM J. Numer. Anal.*, 39:1343–1365, 01 2002.
- [22] M. Gander. Private communication, 2024.
- [23] Martin J. Gander. Schwarz methods over the course of time. *Electronic Transactions on Numerical Analysis*, 31:228–255, 2008.
- [24] Martin J. Gander and Soheil Hajian. Analysis of Schwarz methods for a hybridizable discontinuous Galerkin discretization. *SIAM Journal on Numerical Analysis*, 53(1):573–597, 2014.
- [25] Martin J. Gander and Soheil Hajian. Analysis of Schwarz methods for a hybridizable discontinuous Galerkin discretization: The many-subdomain case. *Mathematics of Computation*, 87(312):1635–1657, 2018.
- [26] R. Glowinski and A. Marrocco. Analyse numérique du champ magnetique d’un alternateur par elements finis et sur-relaxation ponctuelle non lineaire. *Comput. Methods Appl. Mech. Engrg.*, 3:55–85, 1974.
- [27] J. Gopalakrishnan and G. Kanschat. A multilevel discontinuous Galerkin method. *Numer. Math.*, 95(3):527–550, 2023.
- [28] Alexander Heinlein and Martin Lanser. Additive and hybrid nonlinear two-level Schwarz methods and energy minimizing coarse spaces for unstructured grids. *SIAM J. Sci. Comput.*, 42(4):A2461–A2488, 2020.
- [29] G. Karypis and V. Kumar. *METIS – A Software Package for Partitioning Unstructured Graphs, Partitioning Meshes, and Computing Fill-Reducing Orderings of Sparse Matrices*, 2011.
`<\protect\vrule width0pt\protect\href{http://glaros.dtc.umn.edu/gkhome/metis/metis/overview}{htt`
- [30] Hyea Hyun Kim, Eric T. Chung, and Chak Shing Lee. A BDDC algorithm for a class of staggered discontinuous Galerkin methods. *Comput. Math. Appl.*, 67(7):1373–1389, 2014.

- [31] Piotr Krzyżanowski. On a nonoverlapping additive Schwarz method for h - p discontinuous Galerkin discretization of elliptic problems. *Numerical Methods for Partial Differential Equations*, 32(6):1572–1590, 2016.
- [32] Jan Mandel. Hybrid domain decomposition with unstructured subdomains. In Jan Mandel, Charbel Fkrhat, and Xiao-Chuan Cai, editors, *Domain Decomposition Methods in Science and Engineering. Sixth International Conference of Domain Decomposition*, volume 157, pages 103–112. Contemporary Mathematics, 1994.
- [33] *MUMPS: Multifrontal Massively Parallel sparse direct Solver*, 2024. mumps-solver.org.
- [34] Will Pazner and Tzanio Kolev. Uniform subspace correction preconditioners for discontinuous Galerkin methods with hp-refinement. *Communications on Applied Mathematics and Computation*, 4(2):697–727, 2022.
- [35] Alfio Quarteroni and Alberto Valli. *Domain Decomposition Methods for Partial Differential Equations*. Numerical Mathematics and Scientific Computation. Clarendon Press, Oxford, 1999.
- [36] Simone Scacchi. A hybrid multilevel Schwarz method for the bidomain model. *Computer Methods in Applied Mechanics and Engineering*, 197(45-48):4051–4061, 2008.
- [37] Iain Smears. Nonoverlapping domain decomposition preconditioners for discontinuous Galerkin approximations of Hamilton–Jacobi–Bellman equations. *Journal of Scientific Computing*, 74(1):145–174, 2018.
- [38] Andrea Toselli and Olof Widlund. *Domain decomposition methods—algorithms and theory*, volume 34 of *Springer Series in Computational Mathematics*. Springer-Verlag, Berlin, 2005.
- [39] Xuemin Tu and Jinjin Zhang. BDDC algorithms for advection-diffusion problems with HDG discretizations. *Comput. Math. Appl.*, 101:74–106, 2021.